

The

Meteorological Magazine

July 1991

Sensitivity tests for road surface temperature prediction
Estimating fluctuations in pollutant concentration



Met.O 998 Vol. 120 No 1428

© Crown copyright 1991.

First published 1991



The Meteorological Magazine

July 1991
Vol. 120 No. 1428

551.525.2:551.509.314:625.7

Spectral analysis and sensitivity tests for a numerical road surface temperature prediction model

J.E. Thornes and J. Shao
University of Birmingham

Summary

Spectral analysis and sensitivity analysis are used to discover which meteorological input parameters and road thermal properties are most important to a road surface temperature prediction model. The results show that the model is most sensitive to air temperature and cloud cover, and not very sensitive to road thermal properties.

1. Introduction

Numerical road ice prediction models have successfully reproduced the major features of road surface conditions (Thornes 1984, 1989, Rayer 1987, Shao 1990). However, few studies, if any, have looked at the interrelationships between road surface temperature and the geographical, road construction and meteorological inputs to the models, for instance as shown in Table I. How does the output of a numerical model respond to the model parameters and model input, whose values usually cover a considerable range? Spectral analysis and sensitivity analysis are used in this paper in order to answer some of these questions.

Some general research has been carried out relating road surface temperatures to topography and certain weather parameters, such as the influence of topography and wind on the variation of minimum air temperatures and road surface temperatures (Tabony 1985, Bogren and Gustavsson 1988, Gustavsson 1990). Weather conditions have been classified for convenience into damped, intermediate and extreme days by Thornes (1989). Farmer and Tonkinson (1989) have looked at the sensitivity of the Meteorological Office model (Rayer 1987) to road thermal properties and road surface albedo. These researches have shown the value of

Table I. Parameters that control road surface temperature

Geographical	Road construction	Meteorological
Latitude	Depth of construction	Solar radiation
Altitude	Thermal conductivity	Terrestrial radiation
Topography	Thermal diffusivity	Air temperature
Sky view	Emissivity	Cloud cover
Land use	Albedo	Wind velocity
Pollution	Traffic	Humidity
Roughness length		Precipitation
De-icing chemical		

investigating the interaction and sensitivity of road surface temperatures to their environment, but they lack sufficient systematic and quantitative information for model users, and especially for modellers who wish to improve their model predictions. This paper aims to examine the importance of the meteorological inputs and road thermal properties in order to further our understanding of the problems involved.

A method of cross-spectral analysis is used to explore the cross-correlations between road surface temperatures and several meteorological parameters. Then a variety of sensitivity tests are carried out using the Icebreak model (Shao 1990) to examine the response of the model output to changes in both meteorological and road thermal properties, illustrating each with results from two control runs with typical values. Such results reflect model variability and provide suggestions to give better operational results, e.g. via a cautious selection of meteorological, road construction and geographical input data.

2. Cross-correlation analysis

As mentioned by Thornes and Shao (1991), model prediction error originates largely from meteorological input parameters, which include air temperature, dew-point, wind speed, cloud amount and type, and rainfall. All of these parameters are considered as random parameters or part of a time series. To examine correlations between road surface temperature and the meteorological parameters over different time-scales, spectral analysis is used. Details of the method are given in the Appendix.

The results of the spectral analysis are listed in Tables II and III. There are 456 sets of hourly observations from Chapman's Hill on the M5 motorway including road and air temperatures, relative humidity and wind speed. The maximum lag considered in Table II is 24 hours. The number of cloud observations is 129, and the maximum lag considered in Table III is also 24 hours. In these tables, T is the periodicity in hours; $C^2(T)$ is the coherence squared for each time-period (coherence measures the degree of

correlation between two time-series) and $L(T)$ is the time difference of two time-series on the cycle of T th periodicity in hours. The asterisk (*) in these tables indicates that the coherence passes the significance test at either a significance level of 0.01 (Table II) or 0.05 (Table III).

The results show that road surface temperature (T_r) has a close relationship with all the meteorological parameters except cloud cover on a half-day (12-hour) cycle. The small values in $L(T)$ indicate that the variation of T_r responds to that of meteorological parameters very quickly. A significant correlation also exists on some other cycles such as daily and 6-hour cycles. The results show that the air temperature is the most important factor to which road surface temperature responds. When there is a negative phase-difference the air temperature changes are driving the road surface temperatures (e.g. 6- and 16-hour lag), whereas with a positive value of phase difference the road surface temperature is driving air temperature changes (e.g. 8- and 24-hour lag). The lags are not simple to interpret in physical terms due to the effect of traffic, but basically one would expect that the lags should be positive during the day when the road is likely to be warmer than the air, and the opposite at night.

3. Sensitivity tests for meteorological inputs

The most reliable information about the physical nature of the variation of road surface temperature is obtained by actual measurement. Such an experimental investigation is expensive on time and resources and, in most cases, impossible. For instance one would have to wait a long time to measure all cloud combinations at a given wind speed. Sensitivity analysis, by using a mathematical and physical model, is a valuable way to quickly gain an insight into the controlling aspects of the variation of road surface temperature and to develop confidence in model predictions. The Icebreak model is run with standard meteorological observations (for the so-called control runs) for 4 December 1987 and 24 February 1988, representing a 'damped' day and an

Table II. Results of cross-power spectrum analysis between road surface temperature ($X_r(t)$) and meteorological parameters ($X_k(t)$) for Chapman's Hill, winter 1987/88, 456 samples

T hour	Air temperature		Humidity		Wind speed	
	$C^2(T)$	$L(T)$	$C^2(T)$	$L(T)$	$C^2(T)$	$L(T)$
24.0	0.669*	0.44	0.163	-2.39	0.067	1.73
16.0	0.619*	-0.79	0.096	2.19	0.005	2.47
12.0	0.744*	0.08	0.386*	0.35	0.277*	0.38
8.0	0.569*	0.72	0.199	0.99	0.021	-1.16
6.0	0.588*	-0.70	0.267*	-0.76	0.183	-0.50
4.0	0.115	-0.24	0.020	-0.22	0.129	-0.23
3.0	0.147	-0.30	0.296*	-0.24	0.043	-0.33
2.0	0.375*	0.02	0.161	0.24	0.129	-0.05

* see text for further explanation

Table III. Results of cross-power spectrum analysis between road surface temperature ($X_r(t)$) and cloud cover ($X_k(t)$) for Chapman's Hill, winter 1987/88, 129 samples

T hour	Cloud amount		Cloud type	
	$C^2(T)$	$L(T)$	$C^2(T)$	$L(T)$
24.0	0.249*	-0.22	0.197	0.49
20.0	0.106	0.23	0.048	0.35
15.0	0.210	0.83	0.013	-1.04
12.0	0.156	-0.34	0.057	-0.02
10.0	0.310*	0.57	0.048	-0.18
8.0	0.095	0.26	0.132	0.62
6.0	0.554*	0.22	0.071	-0.06

* see text for further explanation

'extreme' day. Figs. 1 and 2 show the results of model prediction with standard input.

In the tests, each of the input parameters (air temperature, dew-point, wind speed, cloud amount and cloud type) is varied through a range of values and all other parameters are held constant. The range of values shown here for each parameter are added or subtracted for each 3-hour input. The model is run from noon to noon and input values are supplied for 1500, 1800, 2100, 0000, 0300, 0600, 0900 and 1200hrs:

- (a) Air temperature: $\pm 1^\circ\text{C}$: the results are shown in Figs 3 and 4.
- (b) Dew-point: $\pm 1^\circ\text{C}$ (Figs 5 and 6).
- (c) Wind speed is the most variable atmospheric parameter considered. In the test, it undergoes a ± 3 kn change which is in accordance with typical forecast input errors (see Thornes and Shao (1991)). Figs 7 and 8 show the results.
- (d) Cloud amount: ± 1 okta when the amount is less than 8 oktas (Figs 9 and 10).
- (e) Cloud type: ± 1 cloud type (1 = low cloud to 3 = high cloud) where appropriate (Figs 11 and 12).

The results of the test runs are displayed in Tables IV and V, and compared with the control runs. The bias, standard deviation (SD) and difference of minimum surface temperatures ($DT(\text{min})$) are given in the tables. The running difference shown in the tables is given by:

$$\text{running difference} = V_m - V_c$$

where V_m is the bias, or SD, or $DT(\text{min})$ with modified input, and V_c is that of control run.

It is seen from the tables that of all of these meteorological parameters, air temperature is the most

important. A change of $\pm 1^\circ\text{C}$ in air temperature results in an extra error of about $\pm 0.8^\circ\text{C}$ in the road surface temperature bias and minimum road surface temperature. This result accords with that of the spectral analysis discussed above. Cloud cover is the second most important factor. Its impact on the model predictions, especially on the prediction of minimum surface temperature, is as expected. The impact of wind speed is small and it is greater on an 'extreme' day than on a 'damped' day. Dew-point seems to only have a minor influence on model output.

4. Sensitivity tests for road thermal properties

It is very difficult to obtain accurate values for the thermal properties of a road construction. Firstly, if sample cores are taken from a road to be analysed in the laboratory, inevitably water is needed to cool the diamond cutter. Water contamination in the sample is impossible to correct for, and significantly affects the thermal properties of the sample. Secondly, the depth of the sub-layers below the surface is often unknown, and therefore one has to make assumptions about the overall thermal properties of a road structure including the sub-base. Hence one has to take published data from the literature and select sensible values for the particular road being dealt with. Model runs are then used to test the sensitivity of road surface temperature to the thermal properties of the road construction.

Table VI shows the typical values of road thermal properties used by several authors. The thermal properties of asphalt, concrete and soil are also unlikely to be the same at different sites, but inevitably the same values have to be used. It can be seen that in general the

Table IV. Results of sensitivity tests for meteorological parameters and comparison to standard results for Chapman's Hill, 4 December 1987

Tests	Output of tests			Running difference		
	Bias	SD	$DT(\text{min})$	A	B	C
Standard	0.15	0.289	0.00	—	—	—
$T_a (+1)$	0.86	0.287	0.74	0.71	0.00	0.74
$T_a (-1)$	-0.64	0.266	-0.81	-0.79	-0.02	-0.81
$DP (+1)$	0.15	0.288	0.03	0.00	0.00	0.03
$DP (-1)$	0.05	0.246	-0.16	-0.10	-0.04	-0.16
$WS (+3)$	0.07	0.278	0.01	-0.08	-0.01	0.01
$WS (-3)$	0.24	0.313	0.04	0.09	0.02	0.04
$CA (+1)$	—	—	—	—	—	—
$CA (-1)$	0.04	0.466	-0.27	-0.11	0.18	-0.27
$CT (+1)$	-0.14	0.432	-0.48	-0.29	0.14	-0.48
$CT (-1)$	—	—	—	—	—	—

Key: T_a — air temperature ($^\circ\text{C}$)
 DP — dew-point ($^\circ\text{C}$)
 WS — wind speed (kn)
 CA — cloud amount in oktas
 CT — cloud type (0 = no cloud, 1 = low cloud, 2 = medium cloud and 3 = high cloud)
A — difference of mean errors
B — difference of standard deviations
C — difference of minimum surface temperature errors

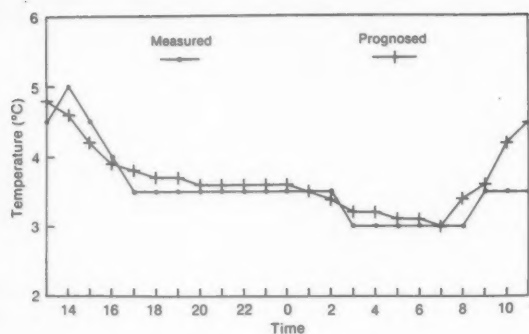


Figure 1. Output with standard input for Chapman's Hill 4 December 1987.

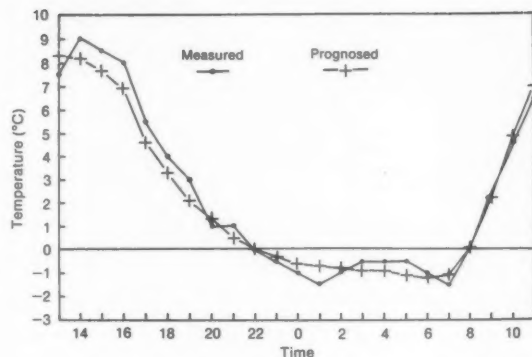


Figure 2. Output with standard input for Chapman's Hill 24 February 1988.

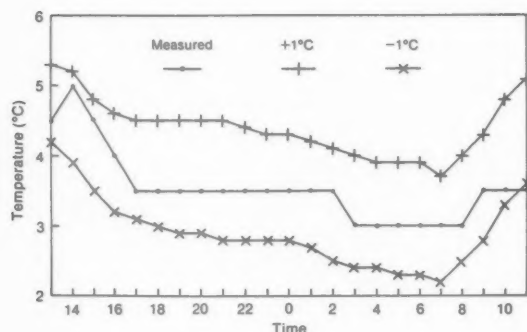


Figure 3. Output with changes in air temperature for Chapman's Hill 4 December 1987.

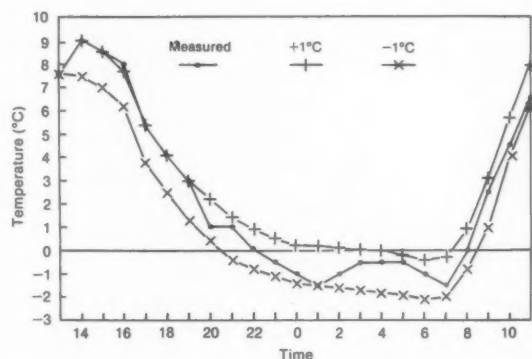


Figure 4. Output with changes in air temperature for Chapman's Hill 24 February 1988.

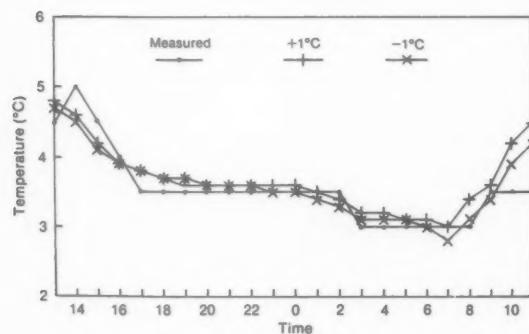


Figure 5. Output with changes in dew-point for Chapman's Hill 4 December 1987.

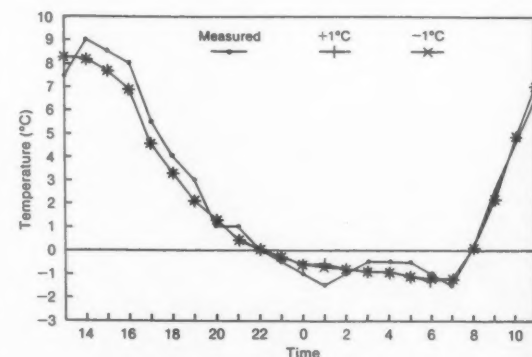


Figure 6. Output with changes in dew-point for Chapman's Hill 24 February 1988.

conductivity of asphalt is lower than that of concrete, and that heat capacity varies less than conductivity.

For this sensitivity analysis the Icebreak model is run with a range of $\pm 20\%$ of the thermal parameters. The road construction is assumed to be: the top sub-layer (0–10 cm asphalt), the middle sub-layer (10–40 cm concrete) and the bottom sub-layer (40–100 cm soil or granite). Table VII shows the values of conductivity and

capacity of asphalt, concrete and soil (or granite) used in the sensitivity tests.

In Table VII, tests (a)–(b) and tests (c)–(d) are for a change of conductivity and capacity of asphalt and concrete, test (e) is for sandy soil and test (f) is for granite. The results of the tests are compared with those of the standard input in Tables VIII and IX. Comparing the model predictions of the control runs to those of the

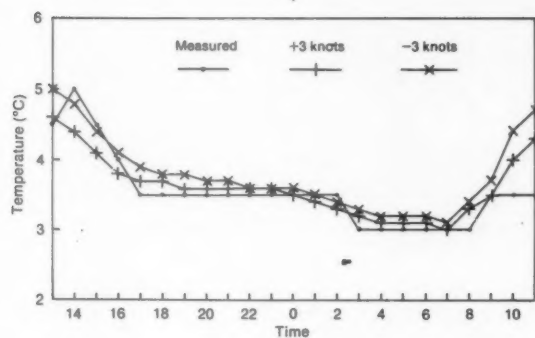


Figure 7. Output with changes in wind speed for Chapman's Hill 4 December 1987.

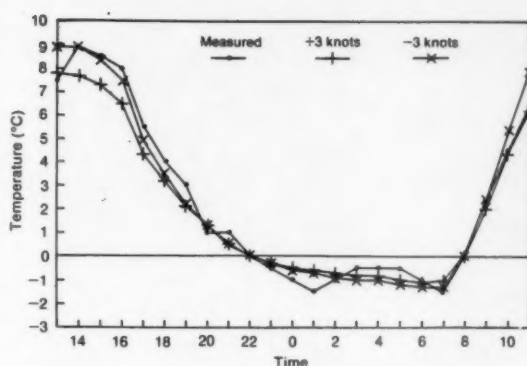


Figure 8. Output with changes in wind speed for Chapman's Hill 24 February 1988.

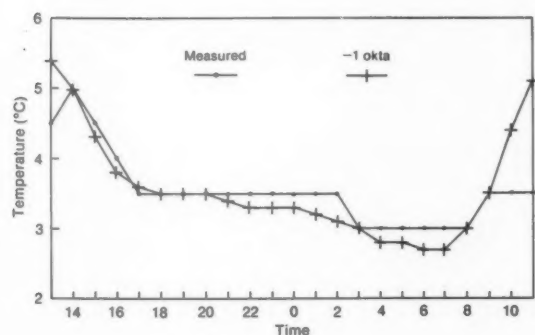


Figure 9. Output with changes in cloud amount for Chapman's Hill 4 December 1987.

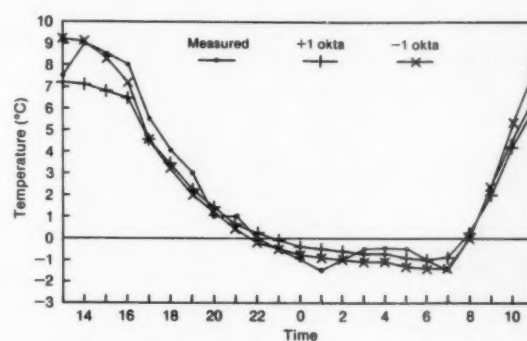


Figure 10. Output with changes in cloud amount for Chapman's Hill 24 February 1988.

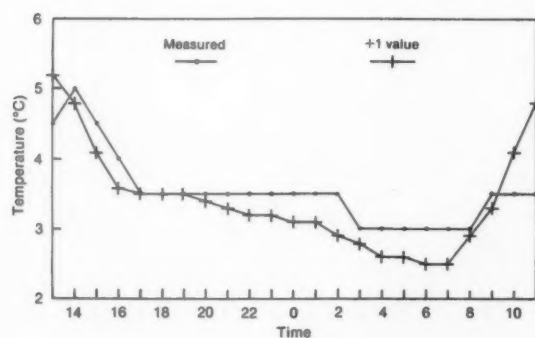


Figure 11. Output with changes in cloud type for Chapman's Hill 4 December 1987.

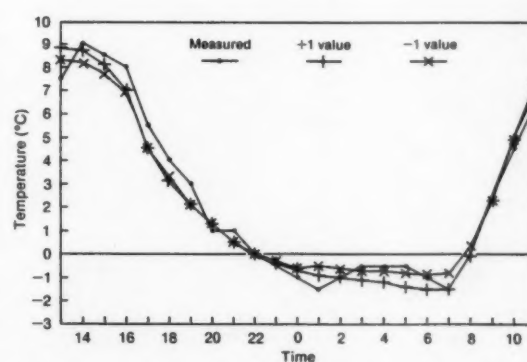


Figure 12. Output with changes in cloud type for Chapman's Hill 24 February 1988.

modified runs, it can be seen that a 20% change of conductivity or capacity of the road sub-layers does not significantly influence model output.

5. Conclusions

Of the many factors that influence the variation of road surface temperature, air temperature is the most important. In routine operation of an ice prediction

model when forecast meteorological input is provided, any error in the forecast of air temperature will result in a similar error in model road surface temperature prediction.

Cloud cover (i.e. cloud amount and cloud type) is another key factor governing the variation in road surface temperatures. On an 'extreme' day, the road surface temperature responds quickly to a change of

Table V. Results of sensitivity tests for meteorological parameters and comparison to standard results for Chapman's Hill, 24 February 1988

Tests	Output of tests			Running difference		
	Bias	SD	DT(min)	A	B	C
Standard	-0.16	0.573	0.30	—	—	—
T_a (+1)	0.68	0.571	1.14	0.84	0.00	0.84
T_a (-1)	-0.99	0.568	-0.57	-0.83	-0.01	-0.87
DP (+1)	-0.16	0.571	0.23	0.00	0.00	0.07
DP (-1)	-0.17	0.567	0.26	-0.01	-0.01	-0.04
WS (+3)	-0.28	0.638	0.37	-0.12	0.07	0.07
WS (-3)	0.02	0.615	0.17	0.18	0.04	-0.13
CA (+1)	-0.28	0.738	0.48	-0.12	0.17	0.18
CA (-1)	-0.09	0.687	0.08	0.07	0.11	-0.22
CT (+1)	-0.18	0.620	-0.04	-0.02	0.05	-0.34
CT (-1)*	-0.06	0.600	0.55	0.10	0.03	0.25

* Only the values of cloud type at 0000, 0300 and 0600 UTC are changed.

Key — see Table IV.

Table VI. Typical values of thermal properties of road materials

Source	Substance	Conductivity $\text{W m}^{-1} \text{K}^{-1}$	Heat capacity $10^6 \text{ J m}^{-3} \text{K}^{-1}$
Farmer and Tonkinson (1989)	Asphalt: wearing	1.40	2.1
	basecourse	1.00	2.1
	roadbase	1.00	2.0
	sub-base	1.25	1.9
	subsoil	1.30	2.5
	Concrete: roadbed	2.60	2.4
	sub-base	1.25	1.9
	subsoil	1.30	2.5
Thornes (1984)	Asphalt	1.30	1.855
	Concrete	2.01	1.675
Oke (1987)	Asphalt	0.75	1.940
	Concrete: dense	1.51	2.11
McCabe and Thompson (1989)	Individual B-road:		
	laboratory	1.40	1.73-2.49
	field	0.97-1.48	1.59-2.40
	Multi-layer road:		
	unfrozen	0.88-1.09	1.77-2.10
	dry ground	0.63-0.95	—
	wet ground	0.98-1.26	—
Weng <i>et al.</i> (1981)	Loam soil 70% saturated	1.58	3.10

Table VII. Conductivity (k) ($\text{W m}^{-1} \text{K}^{-1}$) and capacity (C_m) ($10^6 \text{ J m}^{-3} \text{K}^{-1}$) of road sub-layers for sensitivity tests

Test	Asphalt		Concrete		Soil (granite)	
	k	C_m	k	C_m	k	C_m
Standard	1.25	1.90	1.30	1.90	1.58	3.10
Test (a)	1.50	1.90	1.56	1.90	1.58	3.10
Test (b)	1.00	1.90	1.04	1.90	1.58	3.10
Test (c)	1.25	2.28	1.30	2.28	1.58	3.10
Test (d)	1.25	1.52	1.30	1.52	1.58	3.10
Test (e)	1.25	1.90	1.30	1.90	0.30	1.28
Test (f)	1.25	1.90	1.30	1.90	2.50	1.89

Table VIII. Results of sensitivity test for road thermal properties for Chapman's Hill, 4 December 1987

Tests	Output of tests			Running difference		
	Bias	SD	DT(min)	A	B	C
Standard input	0.15	0.289	0.00	—	—	—
Test (a)	0.17	0.269	0.10	0.02	-0.02	0.10
Test (b)	0.10	0.307	0.00	-0.05	0.02	0.00
Test (c)	0.18	0.278	0.07	0.03	-0.01	0.07
Test (d)	0.10	0.302	-0.01	-0.05	0.01	-0.01
Test (e)	0.15	0.289	0.04	0.00	0.00	0.04
Test (f)	0.14	0.286	0.02	-0.01	0.00	0.02

Table IX. Results of sensitivity test for road thermal properties for Chapman's Hill, 24 February 1988

Tests	Output of tests			Running difference		
	Bias	SD	DT(min)	A	B	C
Standard input	-0.16	0.573	0.30	—	—	—
Test (a)	-0.10	0.559	0.40	0.06	-0.01	0.10
Test (b)	-0.20	0.590	0.20	-0.04	0.02	-0.10
Test (c)	-0.08	0.560	0.41	0.08	-0.01	0.11
Test (d)	-0.22	0.595	0.14	-0.06	0.02	-0.16
Test (e)	-0.14	0.572	0.30	0.02	0.00	0.00
Test (f)	-0.16	0.567	0.28	0.00	-0.01	-0.02

cloud amount and cloud type. Some error in the forecast and observation of cloud cover is usually unavoidable and is thus one of the major sources of model prediction error.

The influence of dew-point temperature and wind speed are normally small. The impact of wind speed on model output is greater on 'extreme' days than on 'damped' days. A 20% variation in the thermal conductivity and capacity of the layers of road construction and soil has a small impact on model predictions.

Acknowledgements

This research was supported in part by Vaisala TMI, the Strategic Highway Research Program and the British Council. The authors are grateful to Bill Fairman of Vaisala TMI, and J. Kings, J. Hales and R.J. Johnson of the Birmingham University Weather Service (BUWS) for their assistance in data collection.

References

- Båth, M., 1974: Spectral analysis in geophysics. Amsterdam, Elsevier.
- Bogren, J. and Gustavsson, T., 1988: A brief survey of the project — applied climatology, road maintenance and increased traffic safety. SERWEC, Highways Meteorology (newsletter) No. 3.
- Farmer, S.F.G. and Tonkinson, P.J., 1989: Road surface temperature model verification using input data from airfields, roadside sites and the mesoscale model. Bracknell, Meteorological Office, Special Investigations Technical Note No. 60. (Unpublished, copy available from National Meteorological Library, Bracknell.)
- Gustavsson, T., 1990: Variation in road surface temperature due to topography and wind. *Theor Appl Climatol*, **41**, 227–236.
- Koopmans, L.H., 1974: The spectral analysis of time series. New York, Academic Press.
- McCabe, E.Y. and Thompson, D.S., 1989: Thermal properties of multi-layered road structures. Grampian Regional Council, Department of Roads, Report No. C201.
- Oke, T.R., 1987: Boundary layer climates, 2nd edition. London, Methuen.
- Rayer, P.J., 1987: The Meteorological Office forecast road surface temperature model. *Meteorol Mag*, **116**, 180–191.
- Shao, J., 1990: A winter road surface temperature prediction model with comparison to others. (Unpublished PhD thesis, University of Birmingham.)
- Tabony, R.C., 1985: Relations between minimum temperature and topography in Great Britain. *J Climatol*, **5**, 503–520.
- Thornes, J.E., 1984: The prediction of ice formation on motorways. (Unpublished PhD thesis, University of London.)
- , 1989: A preliminary performance and benefit analysis of the UK national road ice prediction system. *Meteorol Mag*, **118**, 93–99.
- Thornes, J.E. and Shao, J., 1991: A comparison of UK road ice prediction models. *Meteorol Mag*, **120**, 51–57.
- Weng, D.M., Chen, J.C., Shen, J.C. and Gao, J.B., 1981: Microclimate and micro-agroclimate. Peking, Agriculture Press.

Appendix

In spectral analysis, phase ($P_{j,k}(l)$) and coherence ($C_{j,k}(l)$) are the most useful parameters for measuring the relationship between two time-series $x_j(t)$ and $x_k(t)$. Here l stands for frequency which is the reciprocal of the length of time (period) for $x(t)$ to go through one complete cycle. The phase and coherence are calculated from the power spectral densities ($f_{j,j}(l)$, $f_{k,k}(l)$), cospectrum ($c_{j,k}(l)$) and quadrature spectrum ($q_{j,k}(l)$) by means of the relations

$$c_{j,k}^2(l) = \frac{c_{j,k}^2(l) + q_{j,k}^2(l)}{f_{j,j}(l) f_{k,k}(l)} \quad (\text{A1})$$

and

$$P_{j,k}(l) = -\arctan(q_{j,k}(l)/c_{j,k}(l)). \quad (\text{A2})$$

The spectral densities, cospectrum and quadrature spectrum in equations (A1) and (A2) are estimated from cross-correlation functions (Koopmans 1974, Báth 1974).

The phase function is simply the difference of phase of the two time-series at frequency l or, more precisely, the phase lead of $x_j(t)$ over $x_k(t)$. In practice it is expressed by a time difference in the form

$$L(l) = \frac{mP(l)}{\pi l}$$

The coherence (coefficient of coherence) has the properties of the absolute value of a correlation at frequency l . In some sense it measures the degree of linear association between the time series $x_j(t)$ and $x_k(t)$.

The significance of coherence is assessed by the statistical variable (Koopmans 1974)

$$F' = \frac{(v-1)C_c^2}{1-C_c^2}$$

where v is calculated from

$$v = \frac{2n - m/2}{m}$$

Here n is a sample number or size, m the maximum lag and C_c a critical value. F' follows the F -distribution with 2 and $2(v-1)$ degrees of freedom. If

$$C_{jk}^2 > C_c^2$$

the coherence is considered to be significant.

551.510.42:551.511.61:628.53

A scheme for estimating fluctuations in concentration of an emitted airborne pollutant

F.B. Smith

Meteorological Office, Bracknell

Summary

A simple practical scheme is presented for estimating the probability of exceeding a prescribed concentration, when averaged over a given time-interval, of a passive pollutant emitted from a finite-sized continuous source. A brief summary of the background theory and typical examples are given, with the option of obtaining the required answers simply using the diagrams presented or, somewhat more accurately, the analytical equations. The method has widespread applications in risk analyses wherever the danger of accidental release of hazardous materials to the atmosphere exists.

1. Introduction

Fig. 1 shows an example of a time-record of concentration in a plume at a point some distance downwind of a continuous point source. It shows that, as expected, the plume must be meandering under the action of eddies that are bigger than the width of the plume, so that the concentration is intermittently zero over short periods whereas at other times the concentration is other than zero, albeit quite variable. This complex behaviour can be very important for many hazardous pollutants. Consider three examples:

(a) The pollutant may be inflammable within a band of concentrations, outside of which either there is insufficient material to maintain ignition or too little oxygen. Consideration of the mean concentration alone might suggest this dangerous band is restricted to a fairly short range downwind. Consideration of the distribution of concentrations, the fluctuations, would however indicate that inflammable concen-

trations could occur over a much greater range of downwind distance.

(b) The pollutant may be toxic (e.g. chlorine gas) and the effective toxicity may increase more rapidly than linearly with concentration c . For example, the toxicity of chlorine is believed to increase like $c^{2.75}$. Thus, whilst consideration of the mean concentration field might suggest it is fairly safe to enter the plume at a given location, in reality, because of the fluctuations, it would be highly dangerous since one breath of chlorine at the concentration of one of the peaks could be fatal. The non-linearity further emphasizes the danger.

(c) Some odours can only be perceived by the human nose above some threshold. The designers of an industrial plant that has some odorous pollutant as a waste product must take into account the likely fluctuations in concentration outside the boundaries

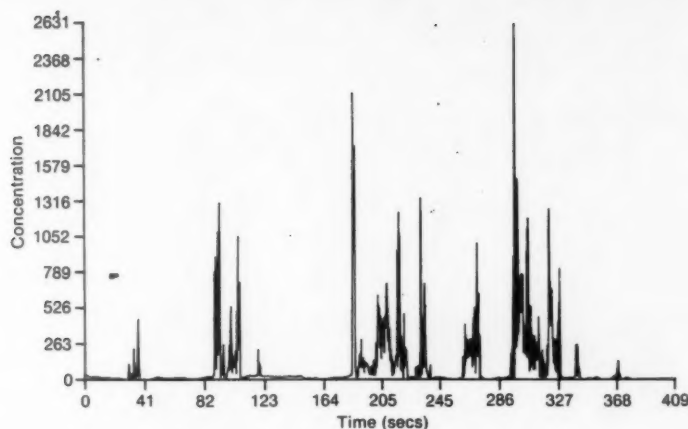


Figure 1. Example of a record of concentration at a point downwind from a point source showing the nature of the concentration fluctuations.

of the plant if they are to avoid a stream of complaints from the public. Rightly, they are not concerned whether the mean concentration can be smelt, but rather whether they can detect the peak concentrations.

Most progress has been made so far in specifying the statistics of the concentration fluctuations with time at a point. However, there is much interest in the spatial distribution of concentration fluctuations. For example, with an inflammable gas, if ignition occurs at some point in the plume where the concentration at the time is within the flammable range it is important to know what is the probability that the flame could travel back along zones of the plume within the range of flammability without any breaks back to the source, or to some location of particular concern (like a home). This is a very difficult problem, although Thomson (1990) has made progress in specifying the nature of spatial covariances of concentration.

2. Available research

It is only within the last 10 years or so that effective research has been directed at this problem, and only now that the beginnings of a practical scheme are emerging. This is the result of complex theory and experimental data. The scheme will no doubt be improved with time, but already it is able to give very useful guidance on the magnitude of the fluctuations and the probability of any concentration being realized at any one time at any downwind position. The background theory will not be given in any detail here. For further details see Sawford (1987), Sykes (1988), Thomson (1990) and Mylne and Mason (1991).

3. The plume and the basic concentration fluctuation parameters

Although the scheme is intended for use with plumes in the atmospheric boundary layer, it will assume

homogeneous isotropic turbulence with an exponential Lagrangian velocity correlation function with finite time-scale τ_L . These assumptions are the easiest to study, and the results provide a useful test case for verifying and developing ideas. Moreover, in the atmosphere, several stages of the plume's development occur before the inhomogeneities become important. At large travel-times the inhomogeneities (or the non-stationariness) always become important so that the user must be wary of the results at long range. Initially we will also assume the source has sufficiently small dimensions that it can be treated as a point source.

If σ_1 is the standard deviation of single particles in the across-wind y direction then

$$\sigma_1^2 = 2A(\exp(-T) - 1 + T) \quad (1)$$

where $A = \sigma_y^2 \tau_L^2$ and $T = t/\tau_L$.

If $\frac{1}{2}\sigma_z^2$ is the variance of the y component of the centroid of a pair of particles taken about the centreline, then

$$\sigma_z^2 = 4A \left[\exp(-T) - \exp\left(-\frac{T}{2}\right) + \frac{T}{2} + \frac{1}{2} \left\{ 1 - \exp\left(-\frac{T}{2}\right) \right\}^2 \right] \quad (2)$$

If $2\sigma_a^2$ is the variance of the y component of the separation of a pair of particles, then

$$\sigma_a^2 = 4A \left[\exp\left(-\frac{T}{2}\right) - 1 + \frac{T}{2} - \frac{1}{2} \left\{ 1 - \exp\left(-\frac{T}{2}\right) \right\}^2 \right] \quad (3)$$

Equations 1-3 satisfy the identity

$$\sigma_a^2 + \sigma_z^2 = 2\sigma_1^2 \quad (4)$$

The forms of these three variances are shown in Fig. 2.

Thomson's random walk studies have supported the following relationship between the concentration fluctuation and the mean concentration at any point on the downwind centreline:

$$\overline{c^2(0)} = \mu \overline{c(0)}^2 \left(\frac{\sigma_1^4}{\sigma_c^2 \sigma_\Delta^2} \right) \quad (5)$$

where $\mu = 1 + 2 \exp\left(-\frac{2\sigma_\Delta}{3\sqrt{A}}\right)$ and where $\overline{c(0)} = \frac{Q}{2\pi u \sigma_1^2}$:

From these relationships we can calculate $\mu \overline{c(0)} A / Q$ and $\sigma_c / \overline{c(0)}$ as functions of t/τ_L , where σ_c is the root-mean-square concentration fluctuation on the centreline given by

$$\sigma_c^2 = \overline{c^2} - \overline{c}^2. \quad (6)$$

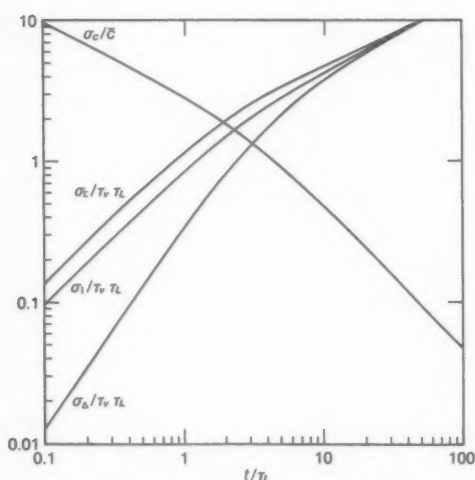


Figure 2. Forms of the three variances defined in the text with $T = t/\tau_L$.

4. The concentration probability density function

Observations made to date indicate that the probability of having a concentration c at any instant is given by the so-called clipped-normal probability density function (PDF)

$$p = \frac{1}{(2\pi)^{1/2} \sigma} \exp\left\{-\frac{1}{2}\left(\frac{c}{\sigma} - \gamma\right)^2\right\}$$

if $c > 0$, or

$$p = \frac{1}{2} \left\{ 1 - \operatorname{erf}\left(\frac{\gamma}{\sqrt{2}}\right) \right\}$$

if $c = 0$, indicating that there is usually a finite fraction of the time, called the intermittency, when the plume is off the centreline and $c = 0$ (note, not all papers define intermittency this way). A clipped-normal distribution

is a Gaussian (or normal) distribution that is centred off the origin, and the part to the right of the origin stands, but the part to the left is integrated and represented by a δ -function of the same magnitude placed at the origin to represent the probability of having zero concentration. This distribution satisfies the requirement that $\int_{-\infty}^{\infty} p(c) dc = 1$. The two parameters σ and γ are determined from

$$\frac{\overline{c}}{\sigma} = \frac{\gamma}{2} \left\{ 1 + \operatorname{erf}\left(\frac{\gamma}{\sqrt{2}}\right) \right\} + \frac{1}{(2\pi)^{1/2}} \exp\left(-\frac{\gamma^2}{2}\right) \quad (7)$$

$$\frac{\sigma_c^2 + \overline{c}^2}{\sigma^2} = \frac{1}{2} (1 + \gamma^2) \left\{ 1 + \operatorname{erf}\left(\frac{\gamma}{\sqrt{2}}\right) \right\} + \frac{\gamma}{(2\pi)^{1/2}} \exp\left(-\frac{\gamma^2}{2}\right) \quad (8)$$

where

$$\operatorname{erf}(x) = \frac{2}{\sqrt{\pi}} \int_0^x \exp(-s^2) ds.$$

Values of $\operatorname{erf}(x)$ are given in Table I.

The values of σ/\overline{c} and γ are determined as functions of σ_c/\overline{c} , which in turn has already been determined as a function of T . Having thus found γ as a function of T , the magnitude of the intermittency I is obtained from the PDF:

$$I = \frac{1}{2} \left\{ 1 - \operatorname{erf}\left(\frac{\gamma}{\sqrt{2}}\right) \right\}. \quad (9)$$

These various functions are plotted in Fig. 3. The variation of σ_c/\overline{c} with T is like $T^{-1/2}$ for $T < 2$ and like T^{-1} for $T > 10$. This can in fact be seen most easily in Fig. 2.

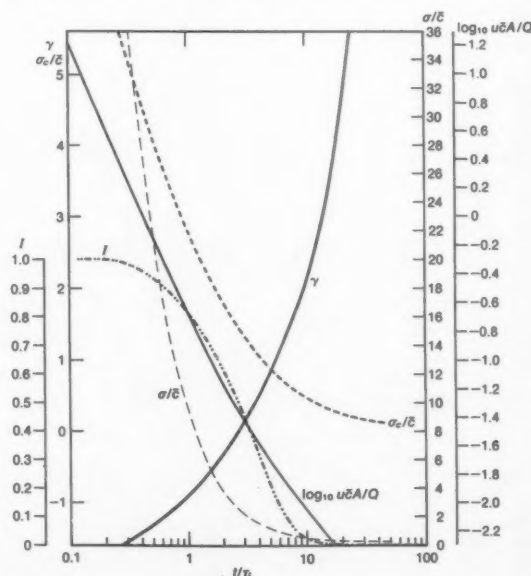


Figure 3. Variation of the concentration fluctuation parameters with travel time on the averaged plume centreline assuming a clipped-normal probability distribution function.

Table 1. The error function erf (*x*) extracted from Jahnke and Emde (1945)

<i>x</i>		0	1	2	3	4	5	6	7	8	9	<i>d</i>
0.0	0.0	000	113	226	338	451	584	676	789	901	013	113
1	0.1	125	236	348	459	569	680	790	900	*009	*118	111
2	0.2	227	335	443	550	657	763	869	974	*079	183	106
3	0.3	286	389	491	593	694	794	893	992	*090	*187	100
4	0.4	284	380	475	569	662	755	847	937	*027	*117	93
5	0.5	205	292	379	465	549	633	716	798	897	959	94
6	0.6	039	117	194	270	346	420	494	566	638	708	74
7	0.7	778	847	914	981	*047	*112	*175	*238	*300	*361	65
8	0.7	421	480	530	595	651	707	761	814	867	918	56
9	0.7	969	*019	*068	*116	*163	*209	*254	*299	*342	*385	46
1.0	0.8	427	468	508	548	586	624	661	698	733	768	38
1	0.8	802	835	868	900	931	961	991	*020	*048	*076	30
2	0.9	103	130	155	181	205	229	252	275	297	319	24
3	0.9	340	361	381	400	419	438	456	473	490	507	19
4	0.95	23	39	54	69	83	97	*11	*24	*37	*49	14
5	0.96	61	73	84	95	*06	*16	*26	*36	*45	*55	10
6	0.97	63	72	80	88	96	*04	*11	*18	*25	*32	8
7	0.98	38	44	50	56	61	67	72	77	82	86	6
8	0.98	91	95	89	*03	*07	*11	*15	*18	*22	*25	4
9	0.99	28	31	34	37	39	42	44	47	49	51	3
2.0	0.995	32	52	72	91	*09	*26	*42	*58	*73	*88	17
1	0.997	02	15	28	41	53	64	75	85	95	*05	11
2	0.998	14	22	31	39	46	54	61	67	74	80	8
3	0.998	86	91	97	*02	*06	*11	*15	*20	*24	*28	5
4	0.999	31	35	38	41	44	47	50	52	55	57	3
5	0.999	59	61	63	65	67	69	71	72	74	75	2
6	0.999	76	78	79	80	81	82	83	84	85	86	1
7	0.999	87	87	88	89	89	90	91	91	92	92	1
8	0.9999	25	29	33	37	41	44	48	51	54	56	3
9	0.9999	59	61	64	66	68	70	72	73	75	77	2

If we suppose that there is some threshold value of *c* above which detrimental consequences occur then the probability *P* that $c > c_*$ (where c_* is this threshold value) is given by

$$P = \frac{1}{2} \left[1 - \operatorname{erf} \left\{ \frac{1}{\sqrt{2}} \left(\frac{c_*}{\sigma} - \gamma \right) \right\} \right]. \quad (10)$$

5. Example

An example may help to see how the scheme can be operated. Suppose $u = 6 \text{ m s}^{-1}$, $\tau_L = 6 \text{ s}$, $\sigma_r = 0.5 \text{ m s}^{-1}$, the source strength $Q = 100 \text{ g s}^{-1}$ and the downwind distance $x = 120 \text{ m}$. What is the probability that the concentration *c* exceeds 200 mg m^{-3} there?

From the given parameters, $A = 9$, $T = 3.333$ and $\mu A/Q = 0.54$. Therefore from equations (1), (2), (3), (5) and (6) or Figs 2 or 3:

(a) $\log_{10} 0.54 \bar{c} = -1.474$. Therefore $\bar{c} = 62.2057 \text{ mg m}^{-3}$.

(b) $\sigma_c/\bar{c} = 1.2431$. Therefore $\sigma_c = 77.35 \text{ mg m}^{-3}$.

Using equations (7), (8) or (9) or Fig. 3 we infer

(c) $\gamma = 0.25106$,

(d) $\sigma/\bar{c} = 1.8623$. Therefore $\sigma = 115.84 \text{ mg m}^{-3}$, where, if Fig. 3 is used, the values of the parameters are found for $T = 3.333$.

The intermittency then works out to be 0.4 and $P(c > c_*) = 7.28\%$.

6. Concentrations off the centreline

The profile of concentration is assumed to be normal in the crosswind direction with standard deviation σ_1 :

$$\bar{c} = \frac{Q}{2\pi u \sigma_1^2} \exp \left(-\frac{y^2 + z^2}{2\sigma_1^2} \right). \quad (11)$$

Thomson's random walk studies indicate that across the plume \bar{c}^2 behaves like

$$\bar{c}^2 = \bar{c}^2(0) (\bar{c}/\bar{c}(0))^q \quad (12)$$

where $q = 2\sigma_1^2/\sigma_c^2$. q is approximately 1 out to $T = 2$ and thereafter slowly increases asymptotically to 2. σ_c is then obtained from $\sigma_c^2 = \bar{c}^2 - \bar{c}^2$. The other parameters can be found exactly as before on the centreline, with the caveat that the value of $P(c_*)$ should be the smaller of that found by the method just described, and that found by assuming that $P(c_*)$ is proportional to the 'mittency' *m* (to coin a new word meaning the opposite of intermittency *I*, i.e. $m = 1 - I$, the fraction of the time spent within the plume).

$$\frac{P(c_*(y))}{P(c_*(0))} = \frac{m(y)}{m(0)}. \quad (13)$$

The value of m can either be found from the method described earlier for points on the centreline, or by $m(y)/m(0) = \overline{c(y)}/\overline{c(0)}$. The two estimates are somewhat different and, although the first method is more accurate, the second is more consistent with the suggested method of finding $P(c_*)$.

In our example consider a point 10 m off the centreline at $x=120$ m. Using equation (11) we get $\overline{c(10)} = 19.2574 \text{ mg m}^{-3}$ and using equations (1), (2), (3), (6) and (12) $\sigma_1^2 = 42.6421$, $\sigma_\Delta^2 = 18.9569$, $\sigma_c^2 = 66.3274$, $q = 1.2858$ and $c^2(10) = 2180.86$, $\sigma_c(10) = 42.5442$, and $\sigma_c(10)/\overline{c(10)} = 2.2092$.

Now we infer γ from equations (7) and (8) since we have σ_c/\overline{c} . Alternatively Fig. 3 can be used for the γ and the remaining parameters using an artificial value of $T=1.49$ corresponding to $\sigma_c/\overline{c} = 2.2092$. Therefore $\gamma = -0.5739$. It follows from equations (7) to (9) that $\sigma = 109.45$, $I = 0.717$, and $P(c > 200) = 0.76\%$, almost one tenth of the value of P on the centreline. Note that the alternative way of estimating P would have given 2.25%, so taking the minimum estimate, the first value stands, although the degree of uncertainty is rather high at these very low values of P .

7. The effect of averaging time

The fluctuations typically have a much smaller time-scale than τ_L . Consequently the peak concentrations may only persist for a relatively short time. The effect of a pollutant, and in particular a toxic pollutant, may be governed by the average concentration in one breath which takes one or more seconds to draw into the lungs. It is expected, then, that the peak averaged concentrations may be significantly smaller than the instantaneous peak concentrations. Random walk simulations suggest that the time-scale τ_f for fluctuations at a point is given by

$$\tau_f = 0.43 \frac{\sigma_\Delta}{u} \quad (14)$$

The effect of averaging over a time t_s is then to reduce the concentration variance according to the equation

$$\frac{\sigma_c^2(t_s)}{\sigma_c^2(0)} = 2 \frac{\tau_L^2}{t_s^2} \left\{ \exp\left(-\frac{t_s}{\tau_f}\right) - 1 + \frac{t_s}{\tau_f} \right\}. \quad (15)$$

In the example we have been following, at 120 m, let $t_s = 1$ s. Then $\sigma_\Delta = 4.354$ and $\tau_f = 0.29$. It follows that $\sigma_c(t_s) = 48.9$. From Fig. 3 we infer $\gamma = 1.0$ and $\sigma = 61$. Hence $P = 0.06\%$, which is clearly a very significant reduction as a result of time averaging.

Thomson has looked at the spatial correlation function for the concentration values. If

$$r = \frac{\overline{c(x)c(x+\Delta)}}{\sigma_c^2}$$

then $r=1$ at $\Delta=0$, and it falls away like

$$1 - A \left(\frac{\Delta}{\sigma_\Delta} \right)^{2\gamma}$$

up to about $\Delta = \sigma_\Delta$, whereafter it behaves like $(\sigma_\Delta/\Delta)^{2\gamma}$ out to at least $\Delta = L$. This slow tail, which is only evident in the longitudinal direction (parallel to the mean wind), he ascribes to inertial meandering of the plume.

8. The effect of source size

The effect of source size is rather complex from a theoretical standpoint. In practice however, its main consequence is to reduce the concentration variance out to $T=1$. This is expected because the finite size must broaden the instantaneous plume and thereby slow down the penetration of 'clean' air into the body of the plume, the process which is responsible for generating internal fluctuations in concentration. Referring back to the section on the concentration fluctuation parameters off the centreline, the finite size (denoted by σ_0) modifies both the formulae for q and $c^2(0)$;

$$q = \frac{\sigma_1^2 + \sigma_0^2}{\sigma_c^2 + \sigma_0^2} \quad (16)$$

and

$$\overline{c^2(0)} = \mu \overline{c(0)}^2 \frac{(\sigma_1^2 + \sigma_0^2)^2}{(\sigma_c^2 + \sigma_0^2)(\sigma_\Delta^2 + \sigma_0^2)}. \quad (17)$$

The consequences are summarized in Fig. 4 where experimental data due to Fackrell and Robins (1982) are compared with Thomson's random walk modelling results. As can be seen in Fig. 4, the larger σ_0 is the smaller is the maximum variance and the further downwind it occurs. These points are further illustrated in Figs 5 and 6.

9. Real situations in the boundary layer

For a source near the ground the assumption of isotropic homogeneous turbulence does not appear very realistic. However, the high frequency turbulence responsible for generating the international spread of the instantaneous plume and its internal concentration fluctuations is virtually isotropic and homogeneous, especially in the earlier stages of the plume's growth. Broadly speaking then, we can assume the plume develops as predicted by isotropic theory until σ_c/\overline{c} is about 1, after which it evolves in a self-similar manner; that is, it is as though t/τ_L becomes constant since, as the plume deepens, so the mean value of τ_L increases.

In very stable conditions, a difficulty arises in specifying the sometimes large meanders of the plume due to intermittent gravity-driven motions as pools of cooler air slide down into hollows and valleys. Likewise some difficulties occur in very unstable conditions due to the complexity of the buoyancy driven motions. Increased research interest is now focused on concentration behaviour in light-wind situations, whether in very unstable or very stable conditions.

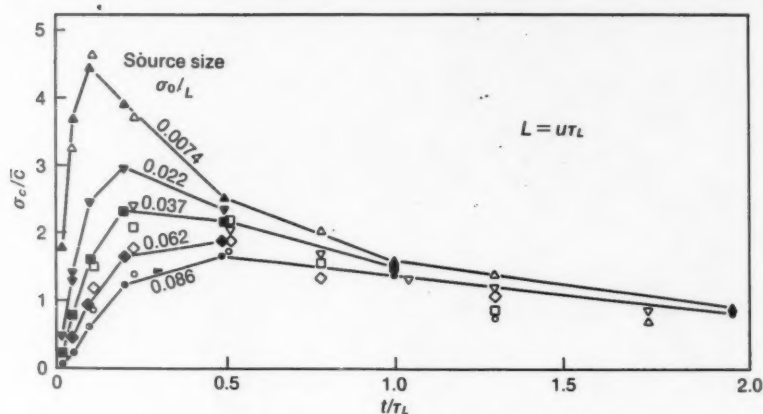


Figure 4. Variation of normalized concentration variance with travel time and with source size. A comparison of theory due to Thomson (1990) (solid symbols), and experimental data due to Fackrell and Robins (1982) (open symbols).

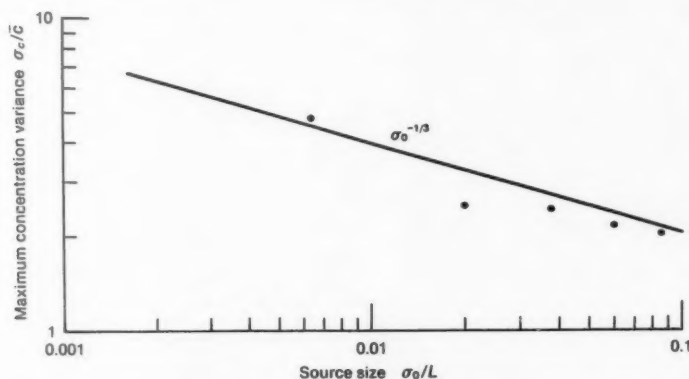


Figure 5. Variation of maximum concentration variance with source size, according to experimental data due to Fackrell and Robins (1982).

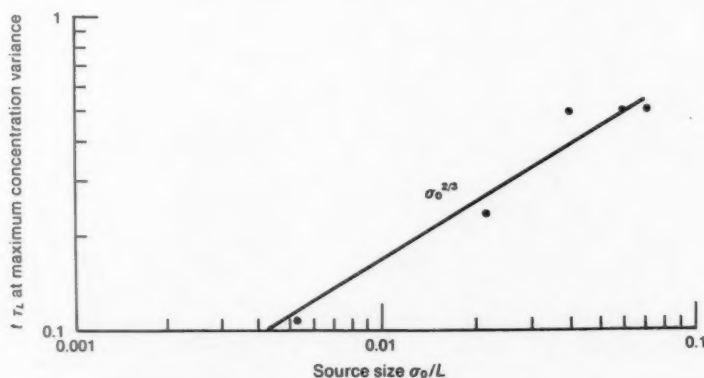


Figure 6. Variation with source size of the travel time at maximum concentration variance (Fackrell and Robins 1982).

10. Fluctuations in concentration at long range

So far we have considered the fluctuations in concentration within a plume from a continuous source out to a distance of perhaps 1 km. Fluctuation analysis also becomes very important at downwind distances much greater than this when the time over which the emission

occurs is smaller than the travel time, or when the synoptic situation changes over a time that is smaller than the travel time. In both these situations it is probable that any receptor only experiences a small part of the possible range of fluctuations. The concentrations the receptor sees, and the risk these may imply, can only be described in statistical terms.

Classically, plumes of debris have always been considered in the same terms as plumes of smoke emanating from a factory chimney. It was recognized that such a plume contains a lot of structure (as we have already seen), blobs and wisps of high concentration surrounded by areas of lower or zero concentration. However, when the plume is averaged over many minutes, these irregularities are largely ironed out and a smoother distribution of concentration is achieved. The plume can then be described in terms of just a few simple parameters. Principal of these are (i) the position of the centroid, or centre of mass, of the plume material (considered as a function of distance downwind from the source), and (ii) the width of the plume (again a function of downwind distance), often expressed as the standard deviation of the concentration distribution about the centroid. In reality the second parameter may be two parameters — the horizontal width and the vertical depth.

Such a description has been used for plumes out to much greater distances than the short distances over which chimney plumes are normally visible. For example the plume from the aluminium smelter at Mt. Isa in Australia has been tracked by instrumented aircraft out to 1800 km in simple meteorological situations when the plume's character can still be described in terms of these few basic parameters (Carras and Williams 1988). They have analysed these measurements in terms of the way the width varies with distance (see Fig. 7).

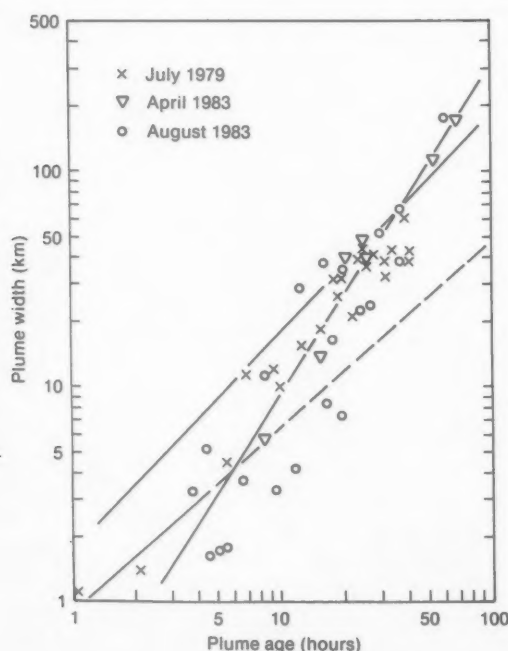


Figure 7. Log-log plot of the measured values of plume width (as a standard deviation) as a function of plume age at Mount Isa, Australia.

However, experience in the atmosphere, as well as modelling studies, suggest that such simple plume ideas are invalid in most meteorological situations after some 20 hours of travel because by that time the plume has grown so wide that synoptic-scale variations in the wind-field can gradually distort and deform the plume into shapes that cannot sensibly be described by the simple parameters described above. In the conditions outlined at the beginning of this section, it is as though we are forced to look at the complex structure of the plume in a similar way as we looked at the instantaneous structure of the plume at very short range in earlier sections of this paper.

This approach has been supported by our experiences with the radioactive-debris plume from the Chernobyl Reactor accident in late April and early May 1986. The resulting depositions, and the consequences they had on the safety of food and on wildlife stimulated many organizations and governments to review the models they had available at that time. Most, if not all of these, were found wanting and this resulted in new, widespread modelling activities. A brief description will now be given of one of these new models, that developed at the Meteorological Office.

11. The UK Nuclear Accident Model

The Meteorological Office has developed a sophisticated random-walk or Monte-Carlo model in order to simulate, in both forecast and hindcast modes, the transport, decay and deposition of radioactive debris emitted from any site in Europe. It is given the acronym NAME (The Nuclear Accident Modelling Exercise). A global version of the model capable of treating emissions from any site in the world will be developed shortly. The plume is simulated by releasing a large number of 'particles' at the source (at hourly intervals, reflecting the emission profile in time and space) and allowing them to be transported by 3-dimensional winds taken from the output of the Meteorological Office's weather forecasting models. When run in the hindcast mode, the 'actual' analysed winds are used from earlier forecast runs rather than forecast winds. A 10-day roll-over archive is used to store past winds for this purpose. A time-step of 15 minutes is used (an appropriate eddy turnover time in the convective boundary layer) and at each step a random perturbation is added to the horizontal displacements (and to the vertical displacements outside the boundary layer) to account for turbulent diffusion:

$$\mathbf{x}_{i+1} = \mathbf{x}_i + \mathbf{u}(\mathbf{x}_i)\Delta t + \mathbf{A}r$$

where Δt is the time-step, r is a random number from the standard normal (Gaussian) distribution and A is a coefficient chosen so that the implied turbulent energy remains quasi-constant in time. Within the boundary layer the particles are randomly reassigned in the vertical at the end of each time-step so that over a period

of time each particle will sample the mean wind at each level. Particles are released from different heights to allow for initial buoyant rise at the source.

The model is multi-level, with a realistically evolving boundary layer, inferred at each hour from the forecasting model output. As its height changes, so particles are entrained and detrained from the layer into the layer above.

A mass of pollutant or radioactivity is associated with each particle at the outset, and concentrations in air are calculated by counting the particles in each grid-volume weighted by the mass they each then carry. If the initial emissions are only coarsely known, comparison of the calculated concentrations can be compared with any field measurements to refine the emissions and the mass each particle carries.

The particle 'mass' is constantly being modified by radioactive decay, by chemical or physical transformations, by dry deposition and by wet deposition. The wet deposition in the model requires a good knowledge of the precipitation field, and this is obtained by inputting the results of a semi-independent programme which combines observations from surface rain-gauges, from weather radar (corrected for false inputs), from satellites and from the weather forecast model's output on rain.

In areas where weather radar output is available the resolution of the rainfall field is as good as 5 km. Even if the model's implied concentrations of pollution in the air contain some errors, at least such a highly resolved

rainfall field will provide valuable information on where heavy depositions of pollution are likely to have occurred; and this is vital to agricultural monitoring teams in situations like Chernobyl. An example of the output of the model is given in Fig. 8. It confirms the distorted and convoluted nature of the plume.

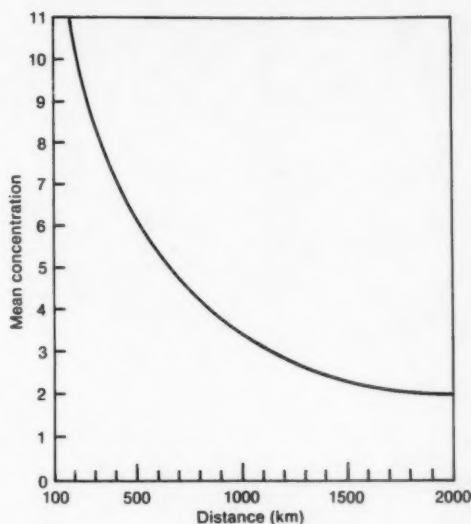


Figure 9. Variation of the mean concentration within plume material as a function of distance. The concentration is equated to the number of particles found in the grid-square (roughly 35 km square) when 200 particles are released per hour.

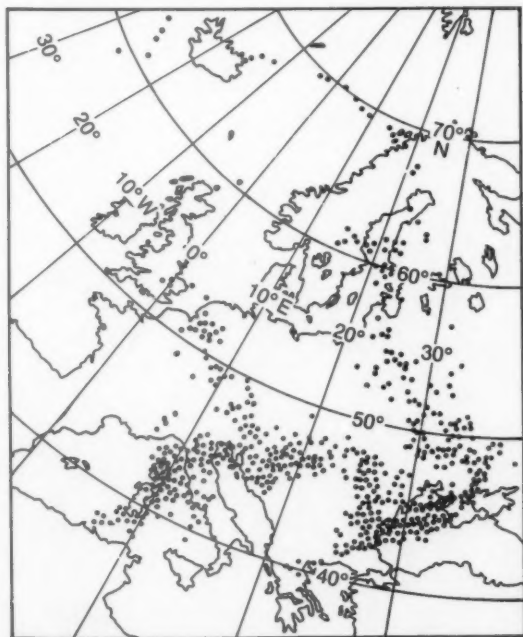


Figure 8. Simulation of the Chernobyl plume at midday on 2 May 1986 using the UK Nuclear Accident Model (NAME). In spite of the relatively few particles simulating the release the model does quite well in indicating the debris over southern Europe and over eastern England.

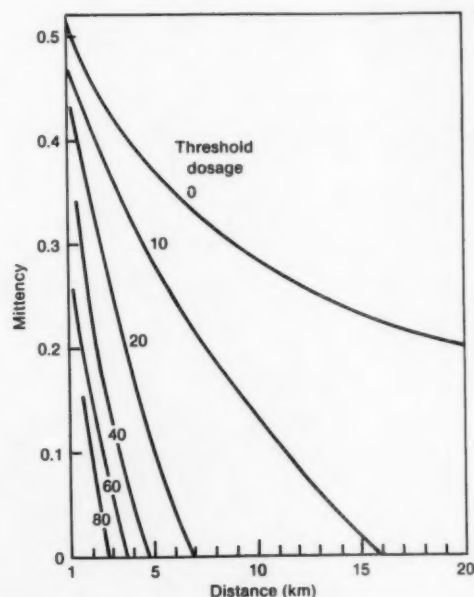


Figure 10. Variation of concentration intermittency (fraction of time the concentration exceeded the given threshold) with distance for several specified threshold dosages. Units of dosage are related to the sum over time of the number of particles in a grid-square in each time-step.

12. Statistical description of a plume at long range

The NAME model has been run on several randomly selected occasions out to 5 days with a continuous release of particles from a specified source located at a gridpoint near the centre of the model area which lies in Cumbria. The plumes grow over these 5 days and show all the distorting features evident in Fig. 8. The following parameters have been determined for both concentrations in the atmosphere, for time-integrated concentrations (or dosages), and for depositions on the underlying surface:

- (a) the mittency of the plume for specified threshold values, i.e. what fraction of the time the concentration exceeded the given threshold,
- (b) the mean concentration or dosage or deposition at specified positions and at specified times after the start of the release, and
- (c) the PDF of the 'observed' concentrations or dosages about their respective means.

This work is not yet finished, but it already shows a degree of order and meaningfulness in its results. For example the distributions in (c) above are very similar to those at short range discussed in earlier sections. It still has to be clarified as to whether the PDF is best represented by the clipped-normal PDF implied at short range, or whether a sample exponential distribution is better

$$p(c) = 1 - \exp\left(-\frac{c}{\bar{c}}\right).$$

Other examples of these preliminary results are shown in Figs 9 and 10.

Acknowledgements

I would like to thank three of my colleagues, Dr D.J. Thomson, Mr K.R. Mylne and Mr R.H. Maryon for their considerable help in the formulation of this paper. Much of the theory behind the method originates from Dr Thomson in the reference given below, and in other unpublished work. Invaluable experimental results supporting the theory come from the work of Mr Mylne. Mr Maryon and his small team has done the majority of the work on the Nuclear Accident Model.

References and bibliography

- Carras, J.N. and Williams, D.J., 1988: Measurements of relative σ_z up to 1800 km from a single source. *Atmos Environ*, **22**, 1061-1069.
- Fackrell, J.E. and Robins, A.G., 1982: Concentration fluctuations and fluxes in plumes from point sources in a turbulent boundary layer. *J Fluid Mech*, **117**, 1-26.
- Jahnke, E. and Emde, F., 1945: Tables of functions with formulae and curves. New York, Dover Publications.
- Mylne, K.R. and Mason, P.J., (1991): Concentration fluctuation measurements in a dispersing plume at a range of up to 1000 m. Submitted to *Q J R Meteorol Soc*.
- Sawford, B.L., 1987: Conditional concentration statistics for surface plumes in the atmospheric boundary layer. *Boundary-Layer Meteorol*, **38**, 209-223.
- Sykes, R.I., 1988: Concentration fluctuations in dispersing plumes. In Venkatram, A. and Wyngaard, J.C. (eds): Lectures on air pollution modeling. Boston, American Meteorological Society.
- Thomson, D.J., 1990: A stochastic model for the motion of particle pairs in isotropic high-Reynolds-number turbulence, and its application to the problem of concentration variance. *J Fluid Mech*, **210**, 113-153.

Notes and news

Fourth Workshop on Operational Meteorology, Whistler, B.C. Canada, 15-18 September 1992

The workshop, sponsored by the Atmospheric Environment Service of Environment Canada and the Canadian Meteorological and Oceanographic Society, will have a principal theme of 'Forecasting in the Nineties'.

The Program Committee wishes to solicit papers on the following topics:

- (a) The meteorological data explosion — the integration and effective use of information in an operational setting.
- (b) Forecast techniques and conceptual models — their place in forecast decision making.
- (c) Climate services — how can they be used effectively.
- (d) Delivery — techniques and requirements to effectively deliver forecasts to the user.

The workshop format will consist of laboratory sessions, submitted papers, invited papers, panel discussions, poster sessions and demonstrations. A brief introduction of each poster session will be made during an appropriate oral session.

Titles and reviewers' abstracts of 400-800 words should be sent to

Neil McLennan
Chairman Program Committee
Atmospheric Environment Service
Suite 200, 1200 West 73rd Avenue
Vancouver B.C.
Canada V6P 6H9

Authors should indicate their preference for presenting their paper orally, in a laboratory or poster session, or as a demonstration. Preferences will be considered to the extent possible. Abstracts will be evaluated on their relevance to the theme as well as on quality. Papers not related to operational meteorology will not be accepted. The deadline for laboratory submissions is 1 October 1991, and for all others is 1 February 1992. Authors will be notified regarding the acceptance of their abstracts and instructions on the format of their papers by 1 November 1991 for laboratories and by 1 March 1992 for other sessions.

Complete camera-ready papers of not more than eight pages, including diagrams, must be received by the Program Chairman no later than 15 June 1992. A pre-print volume will be prepared and distributed to all registered workshop attendees.

For additional information contact either Neil McLennan (Phone: 604-664-9073 Fax: 604-664-9066) or Gerard Neault (604-664-9052).

Reviews

The telemetry of hydrological data by satellite, by I.C. Strangeways. 209 mm × 295 mm, pp. v+60, illus. Wallingford, Institute of Hydrology, 1990. Price £7.00.

This short book, it is only 60 pages long, is a contribution to the Institute of Hydrology Report Series (No. 112). It is softback, and is intended to provide the basic information that a prospective user of satellite telemetry might need in setting up a communications system using facilities offered by both geostationary and polar-orbiting satellites. The author regards the information contained therein as a handbook intended as an introduction to satellite techniques and as an encouragement to use them. He is well placed to write such a document having been involved in developing automatic weather stations and using satellite telemetry for many years.

The information is contained in six chapters covering the Meteosat system, the practical evaluation of a satellite telemetry system, commercial equipment and operating costs, the international situation and conclusions. There are eleven references, of which five are to work reported by the author, and this is an indication that in reading this book one should bear in mind that it represents a rather personal view of satellite telemetry. In spite of this, it is extremely useful in that it sets down much material which is spread widely through a range of literature. The text is clear and easy to read, and most of the diagrams are clear and concise, although some of the data listings have not reproduced well (for example fig. 3.6).

The emphasis throughout is on the Data Collection Platform (DCP) facility provided on the Meteosat series of satellites. The Argos polar-orbiting satellite communications system is mentioned, but there is no mention of commercial VSAT systems, the Meteosat Data Dissemination Mission (MDD) or the ESA CODE experiment based upon the Olympus satellite. Nevertheless the concentration on the systems most used by meteorologists and hydrologists serves to emphasize the practical nature of the book.

A strong argument in favour of using satellite communications is presented, based upon the falling costs of the equipment needed and ease of maintenance, although it is assumed that the costs of any such services in the future will remain free. It is argued that there are a significant number of benefits in using satellite telemetry and these are listed, although it is recognized that the proportion of these benefits with hydrological applications is not known. The reader is referred to 'an authoritative guide' as to the future of satellite telemetry in hydrology obtainable from ESA. It is a pity that this book was produced before the issue of WMO Report

TD No. 256 entitled *'Use of and requirements for satellite imagery and data transmission for hydrological purposes'* by T. Kinoshita (WMO Tech. Reports to the Commission for Hydrology No. 24, 17 pp, 1990). This publication takes the form of a report on a questionnaire. It notes that out of 34 countries who responded 27 did not use satellites for the transmission of hydrological data from data collection platforms, whereas 16 countries said that they had plans to use satellites in this way as follows,

Satellite type: geostationary	11
polar orbiting	9
communication	4.

This information has to be reconciled with that contained in the review publication, which notes on page 11 that in the 1990s it is expected that 5000 DCPs out of a total of 12 500 will be used for the collection of hydrological data. The implication is that most of the usage of DCPs for hydrology may be concentrated in a few countries. At the time the author wrote his book, only 400 stations were registered to use Meteosat and 1800 were registered with the US Geological Survey. This total of 2200 was expected to increase to 12 550. This expected increase is supported by the WMO survey, although the sixfold increase expected by ESA may be too optimistic and a three- or fourfold increase might be more realistic. The sentiment expressed by the author that 'anyone contemplating satellite telemetry for hydrology will probably use a geostationary satellite' (page 13) is not borne out by the WMO survey.

Whilst the majority of the information contained in this book is accurate, and there are useful descriptions of the Meteosat ground segment facilities and message dissemination procedures, there are some inaccuracies and omissions. For example, Eumetsat is not strictly funded by just the member countries of ESA but by the National Meteorological Services. There is no discussion of what causes system downtime, for example satellite decontamination exercises, eclipses, etc. Data distribution and charging policy issues are not discussed. Cost comparisons with UHF and microwave ground telemetry systems are not made recognizing that in the future the acquisition of sub-daily data may not be cost-effective using satellite systems if the service attracts a charge from the satellite operators.

Unfortunately the material contained in this manual will become out of date fairly quickly. For example, some of the information on Meteosat Second Generation is already out of date and the section on commercial equipment likewise. In spite of the limitations noted in this review, the author has assembled a lot of very useful information on satellite telemetry. This manual is an important source of practical data, and should therefore be essential reading for all those contemplating acquiring hydrological and meteorological data via satellites.

C.G. Collier

The hurricane, by R.A. Pielke. 184 mm × 252 mm, pp. xi+228, illus. London, New York, Routledge, 1990. Price £50.00. ISBN 0 41503 705 0.

The hurricane is one of meteorology's most fascinating and awesome phenomena, and its destructive force is seldom appreciated by those living out of the tropics. It is also an excellent example of many important meteorological processes at work — convection and the release of latent heat are essential components of this heat engine, as are the exchanges of sensible heat and moisture at the surface. Hurricane motion, so important to forecast accurately if lives are to be saved, is often irregular and depends not only on the large-scale steering flow in which the system is embedded, but also on its interaction with troughs and jets in middle latitudes. Any book devoted to the subject has to consider extratropical as well as tropical meteorology and has, therefore, plenty of ground to cover.

The author attempts to do just that in a non-mathematical framework which is aimed at the educated layman. The publisher's hand-out describes it as a 'well-illustrated and accessible book providing a state-of-the-art assessment of the climatology, forecasting and physical processes associated with tropical cyclones'. Well illustrated it certainly is, having some 190 pages of figures and diagrams. However, the choice of material is very strange, with over half the book taken up by maps of the tracks of every hurricane in the North Atlantic since 1871; of historical interest perhaps but barely the basis of a well-balanced survey of the subject. If it is to be heavily weighted towards the pictorial, which is not a bad idea for a subject like this, why not have more satellite pictures showing not just the textbook hurricane with an eye, but also the stages of development and the different structures that can occur? There are only three satellite pictures in the book, and all are of a large and fully mature system. The range of topics covered in the text is wide, but the explanation of the meteorology, being condensed into about 30 pages, is necessarily very sketchy. In fact the book gives the impression of being put together rather rapidly with insufficient thought given to clarity of presentation. To take just one example, the reader will be left wondering how the four pages devoted to diagrams showing the mean wind at 850 mb 'demonstrate clearly the validity' of criteria for hurricane development, in the absence of any further explanation. This only goes to show that writing at a level for the educated layman is really far harder than writing for the specialist; clarity is all important as is the ability to appreciate the reader's viewpoint in order to explain what it is that he doesn't understand. In this respect, I am afraid, the book fails.

C.D. Hall

Satellite photographs — 17 May 1991 at 0600 and 1300 UTC

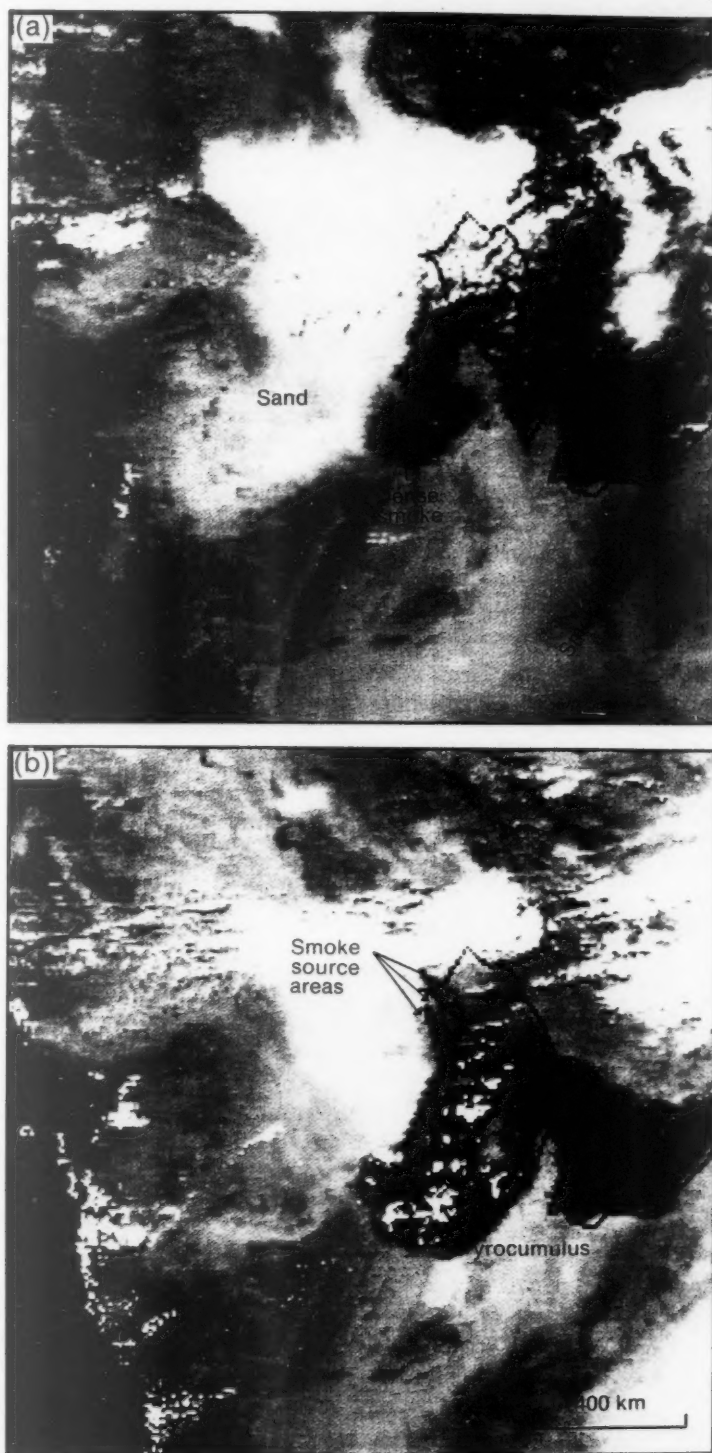


Figure 1. Meteosat visible images of the Persian Gulf area on 17 May 1991 at (a) 0600 UTC and (b) 1300 UTC.

Meteorological satellite imagery of the Persian Gulf area continues to show the effects of the many oil fires that are still burning in Kuwait. The smoke plumes have been seen to extend for many hundreds of kilometres and one example of this can be seen in the images shown here.

The two reprojected visible Meteosat images (Fig. 1) are products from the Meteorological Office's dedicated satellite-image processing system, Autosat-2. They show the type of imagery used within the Nowcasting Section of the Short-range Forecasting Research Division to monitor routinely the extent of the smoke over the Gulf region. This task was initiated in January this year, when smoke was first apparent in satellite imagery.

The plume shown (formed by the smoke from the 500 oil fires reported to be still burning in the area), extended southwards at a rate of 15 kn, consistent with the winds below 850 mb (5000 ft), as shown on the tephigram (Fig. 2).

In the 1300 UTC image (Fig. 1(b)), cumulus clouds can be seen within the smoke area. These have been termed 'pyrocumulus' and form typically during the day in this type of situation. One possible explanation for the formation of these clouds is that the upper layers of

the smoke plume (having an albedo of 5–8%, as measured in recent field studies by the Meteorological Research Flight) absorb solar radiation, causing local heating of the surrounding air and hence strong ascent. In this situation, the unstable atmosphere allowed the developing clouds to penetrate high into the atmosphere, perhaps as high as 300 mb (30 000 ft), as illustrated on the tephigram and as suggested by their low brightness temperatures on the infra-red imagery (not shown here).

These clouds are unlikely to provide a mechanism for the transport of significant quantities of particles into the stratosphere. Firstly, precipitation from these clouds will have washed out the particles (typically between 0.1 and 10 μm) to the surface; secondly, the tropopause is very much higher than 300 mb.

The images show a light grey region covering a large area to the west of Kuwait. Its appearance and movement, combined with the 0600 UTC observations, (Fig. 3) indicate that it was a sandstorm, and was moving at a speed consistent with the observed near-surface winds.

The observations at 0600 UTC within the region covered by the image, reported generally very low visibility, even down to zero at some stations, indicating the extent and severity of the airborne sand and smoke.

G. Holpin and R. Bosworth

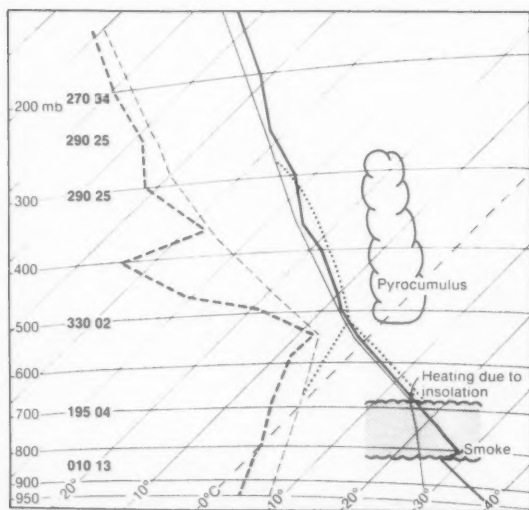


Figure 2. Tephigram for 17 May 1991 at 1200 UTC for King Khaled International Airport (location marked 'K' in Fig. 3), Riyadh, Saudi Arabia (thick lines) (not through plume). Also shown is a schematic showing typical plume depth, and a postulated ascent (thin lines) through the plume (using Kuwait surface data), constructed on the assumption that insolation causes the upper layers of the smoke to behave as if they were a surface, resulting in ascent (dotted line) and cloud formation.

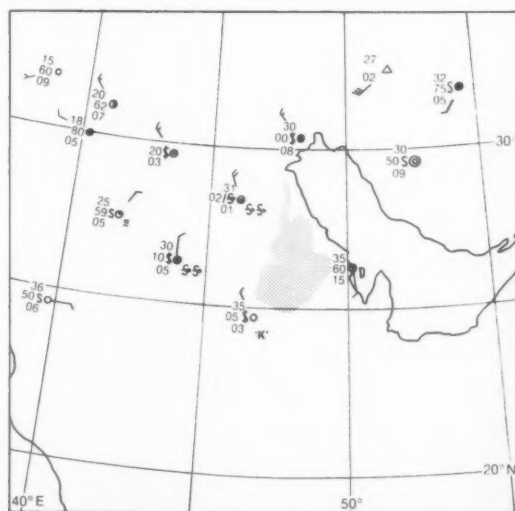


Figure 3. Middle East plotted surface observations on 17 May 1991 at 0600 UTC, with plume area shown stippled.

GUIDE TO AUTHORS

Content

Articles on all aspects of meteorology are welcomed, particularly those which describe results of research in applied meteorology or the development of practical forecasting techniques.

Preparation and submission of articles

Articles, which must be in English, should be typed, double-spaced with wide margins, on one side only of A4-size paper. Tables, references and figure captions should be typed separately. Spelling should conform to the preferred spelling in the *Concise Oxford Dictionary* (latest edition). Articles prepared on floppy disk (Compucorp or IBM-compatible) can be labour-saving, but only a print-out should be submitted in the first instance.

References should be made using the Harvard system (author/date) and full details should be given at the end of the text. If a document is unpublished, details must be given of the library where it may be seen. Documents which are not available to enquirers must not be referred to, except by 'personal communication'.

Tables should be numbered consecutively using roman numerals and provided with headings.

Mathematical notation should be written with extreme care. Particular care should be taken to differentiate between Greek letters and Roman letters for which they could be mistaken. Double subscripts and superscripts should be avoided, as they are difficult to typeset and read. Notation should be kept as simple as possible. Guidance is given in BS 1991: Part 1: 1976, and *Quantities, Units and Symbols* published by the Royal Society. SI units, or units approved by the World Meteorological Organization, should be used.

Articles for publication and all other communications for the Editor should be addressed to: The Chief Executive, Meteorological Office, London Road, Bracknell, Berkshire RG12 2SZ and marked 'For Meteorological Magazine'.

Illustrations

Diagrams must be drawn clearly, preferably in ink, and should not contain any unnecessary or irrelevant details. Explanatory text should not appear on the diagram itself but in the caption. Captions should be typed on a separate sheet of paper and should, as far as possible, explain the meanings of the diagrams without the reader having to refer to the text. The sequential numbering should correspond with the sequential referrals in the text.

Sharp monochrome photographs on glossy paper are preferred; colour prints are acceptable but the use of colour is at the Editor's discretion.

Copyright

Authors should identify the holder of the copyright for their work when they first submit contributions.

Free copies

Three free copies of the magazine (one for a book review) are provided for authors of articles published in it. Separate offprints for each article are not provided.

Contributions: It is requested that all communications to the Editor and books for review be addressed to the Chief Executive, Meteorological Office, London Road, Bracknell, Berkshire RG12 2SZ, and marked 'For Meteorological Magazine'. Contributors are asked to comply with the guidelines given in the *Guide to authors* which appears on the inside back cover. The responsibility for facts and opinions expressed in the signed articles and letters published in *Meteorological Magazine* rests with their respective authors.

Subscriptions: Annual subscription £33.00 including postage; individual copies £3.00 including postage. Applications for postal subscriptions should be made to HMSO, PO Box 276, London SW8 5DT; subscription enquiries 071-873 8499.

Back numbers: Full-size reprints of Vols 1-75 (1866-1940) are available from Johnson Reprint Co. Ltd, 24-28 Oval Road, London NW1 7DX. Complete volumes of *Meteorological Magazine* commencing with volume 54 are available on microfilm from University Microfilms International, 18 Bedford Row, London WC1R 4EJ. Information on microfiche issues is available from Kraus Microfiche, Rte 100, Milwood, NY 10546, USA.

July 1991

Edited by Corporate Communications
Editorial Board: R.J. Allam, R. Kershaw, W.H. Moores, P.R.S. Salter

Vol. 120
No. 1428

Contents

	Page
Spectral analysis and sensitivity tests for a numerical road surface temperature prediction model. J.E. Thornes and J. Shao	117
A scheme for estimating fluctuations in concentration of an airborne pollutant. F.B. Smith	124
Notes and news	
Fourth Workshop on Operational Meteorology, Whistler, B.C. Canada, 15-18 September 1992	133
Reviews	
The telemetry of hydrological data by satellite. I.C. Strangeways C.G. Collier.	133
The Hurricane. R.A. Pielke. C.D. Hall.	134
Satellite photographs — 17 May 1991 at 0600 and 1300 UTC.	
G. Holpin and R. Bosworth	135

ISSN 0026-1149

ISBN 0-11-728858-6



9 780117 288584

